出國報告（出國類別:參加會議發表論文）

海軍軍官學校所屬徐慶瑜助理教授應邀赴美國夏威夷參加美國工程師學會 2009 年第 28 屆海洋、海岸及極地工程國際學術研討會發表論文返國報告

服務機關:海軍軍官學校
姓名職稱:徐慶瑜助理教授
派赴國家:美國
報告日期:98 年 7 月 6 日
出國時間:98 年 5 月 31 日至 6 月 6 日

摘要

本次美國工程師學會2009年第28屆海洋、海岸及極地工程國際學術研討會(ASME 2009 28th International Conference on Ocean, Offshore and Arctic Engineering, OMAE 2009)於5月31至6月5日在美國夏威夷歐胡島舉行，本次會議由美國工程師學會(American Society of Mechanical Engineers, ASME)；特別邀請海洋、海岸及極地工程研究相關之工程技術研究人員與學者參加，與會者約800餘人，大多爲歐美人士，亞洲學者人數較少；本次會議之主題包括：海洋工程、結構安全及可靠度分析、材料技術、計算流體力學研究等，會議分成6天舉行，每場次報告及討論之時間爲二十分鐘，各場次均十分踴躍。

本會議爲國際研究海洋、海岸及極地工程研究應用極爲知名且重要之研討會，目前已舉辦第28屆，歷史悠久；本會議約有800餘位國際知名之人士參加，發表論文達千餘篇；大多爲歐美人士，亞洲以日本、韓國、伊朗及中國大陸均有學者參予，由於主辦單位有多年的研討會承辦經驗，在工作協調上均十分順暢；本次會議申請人發表水下爆炸之研究成果，並於此次研討會中展現海軍軍官學校在此方面之研究能量，與歐美及日本、韓國相關學者利用會議時間及茶會時間充分溝通與討論，獲益良多。

目次

海軍軍官學校出席國際學術會議心得報告

報告人姓名：徐慶瑜
所屬學系：船舶機械工程學系
職稱：助理教授
會議名稱：美國工程師學會 2009 年第 28 屆海洋、海岸及極地工程國際學術研討會(ASME 2009 28th International Conference on Ocean, Offshore and Arctic Engineering, OMAE 2009)
會議時間：2009 年 5 月 31 日至 2009 年 6 月 5 日
會議地點：美國夏威夷
主辦機構名稱：美國工程師學會(American Society of Mechanical Engineers, ASME)
參加會議目的:應邀發表論文
發表論文題目：
中文題目：缺陷加勁圓筒薄殼承受側邊水下爆炸負荷時之暫態反應
英文題目：The transient response of imperfect thin-walled stiffened cylindrical shell exposed to side-on underwater explosion

報告內容：

一、參加會議過程：

1.於2009年5月31日中午1點至會議主辦地點Sheraton Waikiki Hotel 報到，參加之各界的學者專家十分踴躍，本次美國工程師學會2009年第28屆海洋、海岸及極地工程國際學術研討會(ASME 2009 28th International Conference on Ocean, Offshore and Arctic Engineering, OMAE 2009)於5月31至6月5日在美國夏威夷歐胡島舉行，本次會議由美國工程師學會(American Society of Mechanical Engineers, ASME)；特別邀請海洋、海岸及極地工程研究相關之工程技術研究人員與學者參加，與會者約800餘人，大多爲歐美人士，亞洲學者人數較少。

2.本次會議之主題包括：海洋工程、結構安全及可靠度分析、材料技術、計算流體力學研究等，會議分成6天舉行，每場次報告及討論之時間爲二十分鐘，各場次均十分踴躍。

二、與會心得：

本會議爲國際研究海洋、海岸及極地工程研究應用極爲知名且重要之研討會，目前已舉辦第28屆，歷史悠久；本會議約有800餘位國際知名之人士參加，發表論文達千餘篇；大多爲歐美人士，亞洲以日本、韓國、伊朗及中國大陸均有學者參予，由於主辦單位有多年的研討會承辦經驗，在工作協調上均十分順暢；本次會議申請人發表水下爆炸之研究成果，並於此次研討會中展現海軍軍官學校在此方面之研究能量，與歐美及日本、韓國

相關學者利用會議時間及茶會時間充分溝通與討論，獲益良多；本次會議許多學者們均帶領博碩士班研究生參與。

三. 考察參觀活動：
(本次未參加舉辦單位安排之考察活動)

四. 建議：

本次會議許多論文均爲研究生代表報告，與過去均爲教授報告有所不同，以亞洲之日本及中國大陸的研究生而言，用英語發表論文之能力較過去進步良多，台灣之大學，尤其海軍軍官學校，更應注意學生之國際溝通語言能力；同時應鼓勵所屬教師出國發表論文，以增進學校於國際之能見度。

五. 攜回資料名稱及內容：

1.美國工程師學會2009年第28屆海洋、海岸及極地工程國際學術研討會(ASME 2009 28th International Conference on Ocean, Offshore and Arctic Engineering, OMAE 2009)會議議程及摘要
2.美國工程師學會2009年第28屆海洋、海岸及極地工程國際學術研討會(ASME 2009 28th International Conference on Ocean, Offshore and Arctic Engineering, OMAE 2009)會議論文光碟片
3.美國工程師學會2009年第28屆海洋、海岸及極地工程國際學術研討會(ASME 2009 28th International Conference on Ocean, Offshore and Arctic Engineering, OMAE 2009)出席證書。

六. 其他：

無

附錄

Proceedings of the ASME 2009 28th International Conference on Ocean, Offshore and Arctic Engineering
OMAE2009
May 31 - June 5, 2009, Honolulu, Hawaii, USA

OMAE2009-79018

THE TRANSIENT RESPONSE OF IMPERFECT THIN-WALLED STIFFENED CYLINDRICAL SHELL EXPOSED TO SIDE-ON UNDERWATER EXPLOSION

Ching-Yu Hsu*
Department of Marine Mechanical Engineering ROC Naval Academy
Tsoying, Kaohsiung 813, Taiwan, Republic of China

Chan-Yung Jen
Department of Marine Mechanical Engineering ROC Naval Academy
Tsoying, Kaohsiung 813, Taiwan, Republic of China

ABSTRACT

The thin-walled stiffened cylindrical shells are usually applied in a submarine which takes the external pressure load, or in a boiler, pressure vessel or pipeline system which takes the internal pressure load. The thin-walled stiffened cylindrical shells under hydrodynamic loading are very sensitive to geometrical imperfections. This study is investigating an imperfect thin-walled stiffened cylindrical shell(out-of-round ratio is ψ=2%) at a depth of 50m below the water level to see how it withstands sideward TNT 782 kg underwater explosion loading so as to understand its structural transient response. ABAQUS finite element software is used as an analysis tool in the current study, meanwhile, during the analysis process, the Fluid-Structure Interaction (FSI) condition is employed. The structural transient response results of stress and displacement time history of the imperfect thin-walled stiffened cylindrical shell can be used as a reference for the anti-underwater explosion analysis and design of future submersible vehicles, pressure hulls or related structural designs.

Keywords : imperfect stiffened cylindrical shell, underwater explosion

1. INTRODUCTION

Commercial and military vehicles usually adopt stiffened cylindrical shells in the form of a pressure-resistant structure. For military submersible vehicle, in addition to considering water pressure loading, the underwater explosion loading generated during the operation environment should be considered too. When a commercial submersible vehicle is located in an unknown underwater environment, it will unavoidably encounter the impact loading generated during the collision behaviour. Therefore, the nonlinear response generated by the submersible vehicle shell due to such dynamic transient is a very important factor to be considered when performing pressure hull structural design and analysis. Military submarine pressure hull mainly comprises of three traditional pressure hull structures such as: cylinder, dome end and conical pressure hull (as shown in Figure 1).

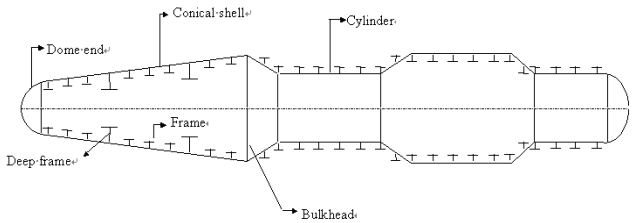

Figure 1. A structural illustration of shell of submarine

Since stiffened cylindrical shell possesses good space planning and volume efficiency in the internal cabinet allocation, it thus occupies most of the space in a pressure hull. The circular cross-section is the best configuration for the stiffened cylindrical shell to resist the external pressure loading. In fact it is impossible for the stiffened cylindrical shell to have circular cross-section configuration owing to the construction technology or the cost. Therefore it goes without saying that this study is very important for the transient response of imperfect thin-walled stiffened cylindrical shell exposed to side-on underwater explosion.

The numerical method for performing explosion analysis can be classified as spatial discretization and surface approximation, which have their own respective advantages and disadvantages. The major advantage of spatial discretization approximation is that it can relatively simulate the reaction between the entire flow field and the structure. Its disadvantage is that it takes

* Assistant Professor and author of correspondence

massive computer memory space and operation time. Its development can be dated back to 1969, Zienkiewicz et al. [1] used finite element method to diverge the structure into stiffness matrix equation, and the fluid motion is represented by Navier-Stokes equation and the solution is found through Galerkin weighted value procedure. In 1978, Marcus [2] used finite element method (NASTRAN) to solve the free vibration reaction of the underwater suspension plate. In 1983, due to the computer operation speed and memory space limitation in the era of 1970-1980, this method is not massively adopted. Until 1990, computer and numerical method was rapidly developed and such method was gradually adopted and used every now and then. In 1995, Huang and Kiddy [3] used finite differential method and Eulerian-Lagrangian descriptive method to solve the transient coupling reaction when underwater spherical casing is facing a vibration wave and bubble impulse. At the same year, Bathe et al. [4] used Arbitrary Lagrangian-Eulerian (ALE) method to solve the coupling issue between fluid and the structural object in the pipeline.

In this study, nonlinear finite element analysis software ABAQUS is used to set up a set of calculation procedures to investigate the transient response of imperfect stiffened cylindrical shell in taking underwater explosion loading effects when fluid structural coupling effect is considered.

2. RESEARCH METHOD

The phenomenon of underwater explosion effect and the theory of fluid and structure coupling effect required in this study are described in the following:

2.1 Phenomenon of underwater explosion effect

During underwater explosions, since energy is released suddenly, high pressure and high temperature gas bubbles and shock waves thus appear suddenly in the water. As the shock wave diffuses outwards, its pressure and speed will drop in a rapid way exponentially. In the gas bubble part, its internal energy will make the bubble to expand outwards in spherical shape, and the peripheral seawater will be pushed outwards. As the bubble expands, its internal pressure will drop accordingly. When maximum volume is reached, the internal pressure in the gas bubble will be minimum, and when this pressure is smaller than the static water pressure it is located, the gas bubble will shrink suddenly. When the shrinkage reaches a limit, the pressure will suddenly rise and secondary pressure wave that are similar to water hammer effect will be generated. This process will appear repeatedly after the start of the explosion, and the peak pressure will get reduced too, and this is the so-called gas pulse or bubble pulse phenomenon as in Figure 2 [5]. The underwater explosion process can generally be divided into three stages: Detonation, Shock wave formation and Propagation, Gas bubble impulse and floating, where in shock wave contains two parts such as the main shock wave formed by the explosion and the secondary pressure wave formed by bubble sphere impulse process. During the outward propagation process of the shock wave, the explosion amplitude gets decayed continuously and the generated explosion loading pressure can be found from the experiment that is a time function of the exponential form [5]. This study only considers the main shock wave loading and the secondary pressure waves are not considered.

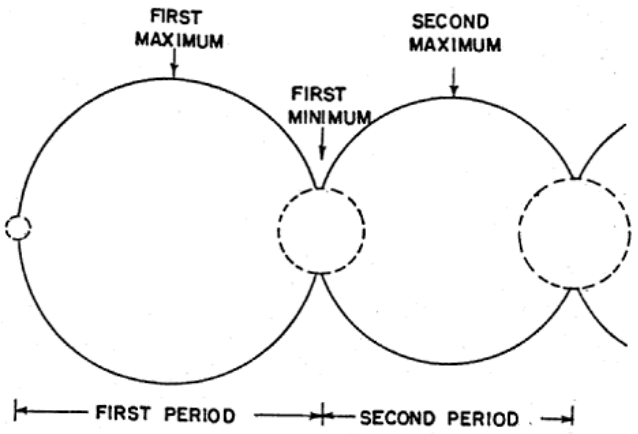

Figure 2. An illustration of the gas bubble impulse process of underwater explosion [5]

2.2 The pressure history function P(t) of main shock wave of underwater explosion

When an explosion starts under the water, the water pressure caused by the shock waves will decay in exponential form with time. At any observation point under the water, the relationship of the shock wave pressure versus time is as shown in the following [5].

$$P(t) = P_m e^{-\frac{t}{\theta}}$$

(1)

$$P_m = K_1 \left(\frac{W^{\frac{1}{3}}}{R} \right)^{A_1}, \theta = K_2 W^{\frac{1}{3}} \left(\frac{W^{\frac{1}{3}}}{R} \right)^{A_2}$$

(2)

P_m : The wave front pressure for shock wave to propagate to the observation point, which is also called the peak pressure; *t*: the time past for shock wave front to reach the observation point, θ: decay time constant. For TNT explosive at different explosive weights W and shock source distance R, the explosive experience constants A_1=1.144, A_2=-0.247, K_1=52.12 and K_2=0.0895 [5].

2.3 Fluid and structure coupling behaviour

When stiffened cylindrical shell takes a shock wave under the water, its structural response, during the analysis, should be considered at the same time as the flow field behaviour surrounding it. This fluid and structure mutual interactive action will continue until the vibration of the structural body decays to a steady state. ABAQUS used Surface-based Interaction Procedure to perform coupling analysis on the nodes of the intimate contact surface between the structure and the fluid, and the detailed analysis process of Surface-based Interaction Procedure is listed in the literature [6]. After the incident shock wave contacts the structure, the reflected pressure wave called scattered pressure wave, should be taken into account in the analysis. The major solving equations are as [7]:

$$M_s \ddot{u} + C_s \dot{u} + K_s u = -[S_{fs}]^T p$$

(3)

$$M_f \ddot{p} + C_f \dot{P} + K_f p = -[S_{fs}]T$$

(4)

$p=p_I+p_S$

(5)

Here *Ms* is the structural mass matrix, *Cs* is the structural damping matrix, *Ks* is the structural stiffness matrix, P_I is the incident shock wave, P_S is the scattered pressure wave and u is the structural displacements. M_f is fluid mass matrix, C_f is fluid damping matrix, K_f is fluid stiffness matrix and S_{fs} is fluid solid coupling transform matrix. The fluid traction T in Eq.(5) is the quantity that describes the mechanism by which the fluid drives the solid.

3. THE TRANSIENT RESPONSE OF IMPERFECT STIFFENED CYLINDRICAL SHELL SUBJECTED TO SIDE-ON UNDERWATER EXPLOSION LOADING

In this work, imperfect stiffened cylindrical shell is used as the target and ABAQUS[6] is used as the tool to investigate the structural response of the case when cylindrical shell subjected to side-on underwater explosion loading with the consideration of structure-fluid coupling effect. The capability verification of ABAQUS in analyzing such problems has been listed in detail in the literature [8-9]. The analysis parameters such as stiffened cylindrical shell, flow field, material mechanical properties and loading conditions are described as in the following.

3.1 The definition of the out-of-round ratio

In this paper the cross-sectional circumference of the stiffened cylindrical shell is assumed to be constant when it becomes imperfect. It is assumed that the cross-section shape of the imperfect stiffened cylindrical shell is oval. The cross-sectional shape of the stiffened cylindrical shell is shown in Figure 3. Here B is the major axis of the oval and R is the radius of cross-sectional area of the ideal stiffened cylindrical pressure.

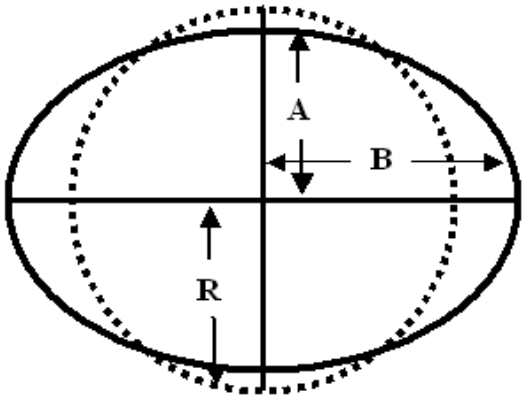

Figure 3. The cross-sectional shape of the ideal and imperfect stiffened cylindrical shell

(Imperfect cross-sectional shape：———)
(Ideal cross-sectional shape：▪▪▪▪▪▪▪▪)

So

$$2\pi \mathrm{R} = 2\pi\sqrt{\frac{1}{2}(A^2 + B^2)}\,,$$

(6)

$$\mathrm{B} = \sqrt{2R^2 - A^2)}\,,$$

(7)

The definition of the out-of-round ratio (ψ)

ψ=[(R-A)/R]×100 %=(1-A/R) ×100 %=(1-η)×100 %

(8)

where

η is the shape transform factor and η=A/R.

3.2 The numerical model of imperfect cylindrical shell with external rib

The stiffened cylindrical shell includes 8 sets of T shape transverse stiffened external ribs with the front and back ends covered with end plates. The length of the stiffened cylindrical shell is L=5040 mm, radius is *R*=2700 mm, shell thickness of the shell is *h*=32 mm, the detailed dimension and geometrical illustration is shown in Figure 4.

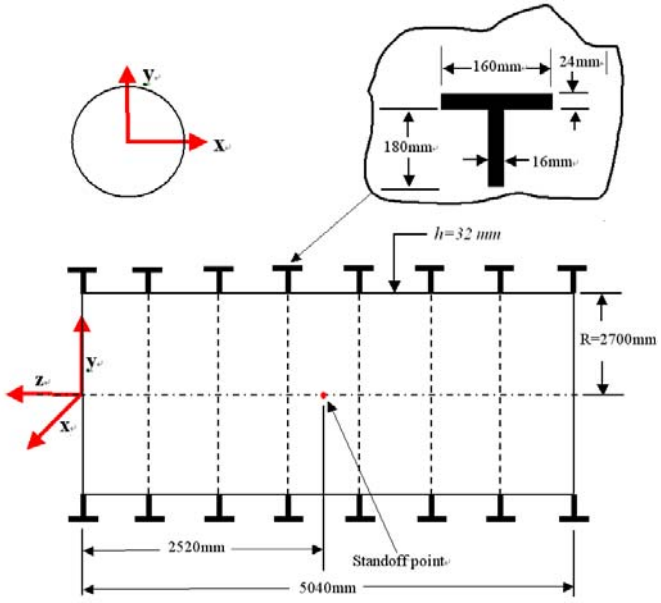

Figure 4. An illustration of the geometrical structure of the stiffened cylindrical shell

There are two models in this study to compare their structured response when subjected to a side-on underwater explosion. One is the Ideal model for which the out-of-round ratio is ψ= 0% and another is the Imperfect model for which the out-of-round ratio is ψ=2%. The finite element models of cylindrical shell and T shape stiffened materials are all simulated by four nodes tetragon double curve thin shell element (element number is S4R). The cylindrical shell part, has 10,656 shell elements and 10,658 nodes. The stiffened rib material part, has 4,608 shell elements and 5,760 nodes. Since the cylindrical shell is subjected to side-on underwater explosion loading, the main shock wave will contact first the shell at the so-called standoff point, which is located at the central location of the neighbouring shock source shell. For the finite element model, the underwater explosion source and the standoff point location of the stiffened cylindrical shell is shown in

Figure 5.

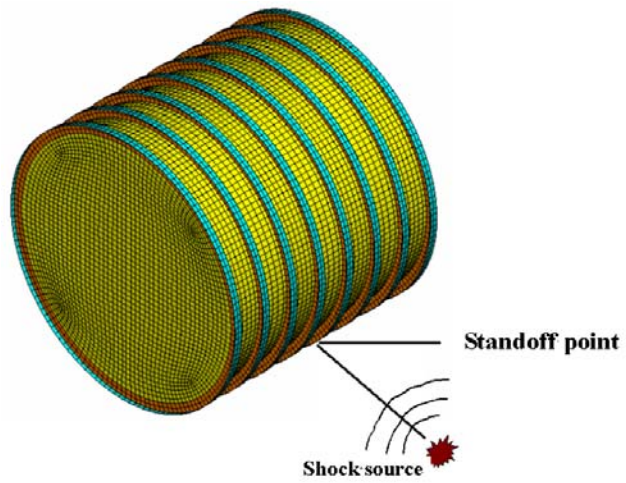

Figure 5. Finite element model of stiffened cylindrical shell

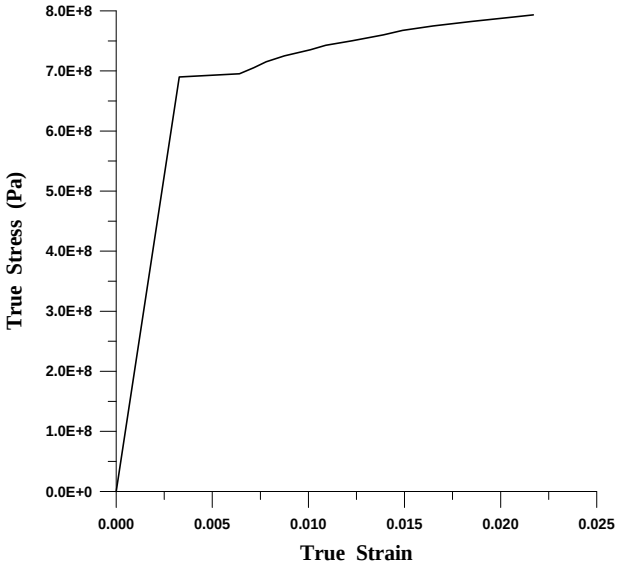

Figure 6. The real stress-strain curve of HY100 steel material [10]

3.3 The mechanical properties of the shell material

The material of stiffened cylindrical shell with external rib is HY100 steel material, which has a elasto-plasticity real stress-strain curve as in Figure 6 [10]. The material mechanical properties are: elastic modulus E=210 GPa, yield strength σ_y=690 MPa, ultimate tensile strength σ_u=793.5 MPa, material density ρ=7828 kg/m^3, Poisson ratio μ=0.29 and elongation rate 18% .

3.4 Underwater flow field

The infinite flow field enclosing stiffened cylindrical shell has its infinite flow field characteristic taken into account through a non-reflected boundary condition. Placed at the outermost boundary of the flow field element area, the entire flow field, including the front and back spherical end, has a horizontal distance of 12.04m and vertical height of 7m. The infinite flow field is simulated using tetrahedron flow element with element number AC3D4, which includes 1,078,779 tetrahedron fluid element and 94,588 nodes. The fluid density is ρw=1,025 kg/m^3, sonic velocity is c=1,519 m/s, and the analyzed underwater flow field finite element model is as shown in Figure 7.

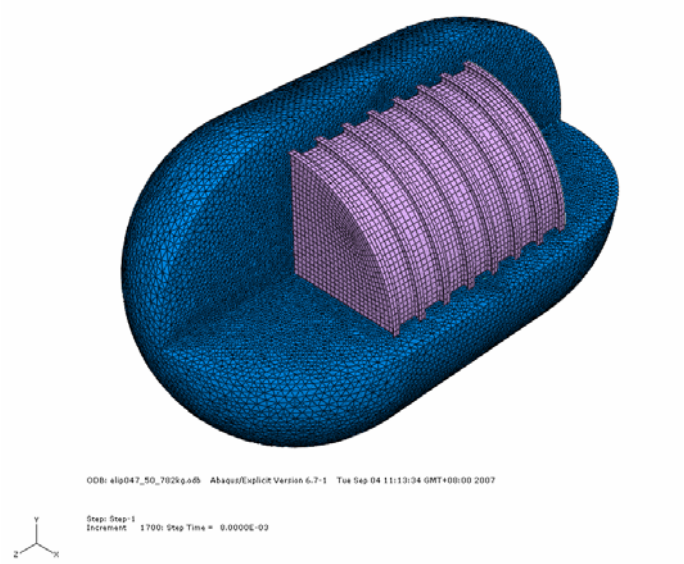

Figure 7. Finite element model of underwater flow field

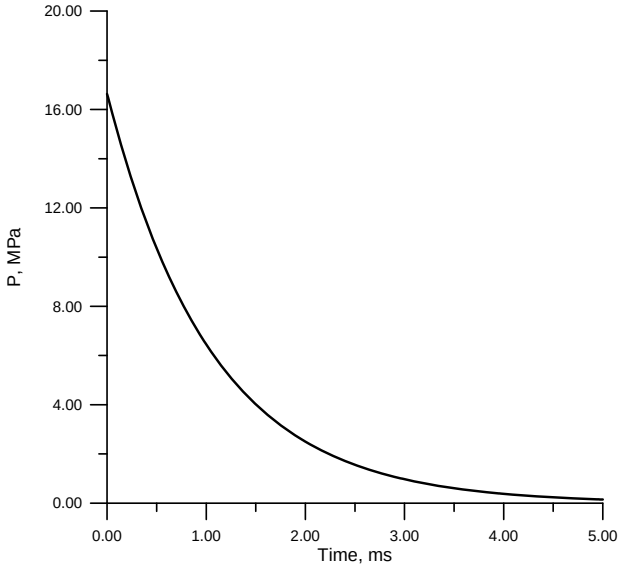

Figure 8. Time history of explosion loading (TNT weight 782kg)

3.5 Loading conditions and boundary conditions

The loading taken by stiffened cylindrical shell in the underwater flow field can be divided into two parts, that is, static water pressure loading and underwater explosion loading.

In this work, stiffened cylindrical shells are placed at flow fields of water depths of 50m respectively, thus they can take static water pressure of 5.02763×10^5 Pa.

Explosive TNT with a weight of 782 kg is selected, the ideal and imperfect stiffened cylindrical shells are placed at water depths of 50m respectively, and the shock source has a distance of 25m from the side of the standoff point (as shown in Figure 5) to perform the explosion effect analysis of the stiffened cylindrical shell structure. The formula of the peak pressure as provided by Cole [5] to perform the explosive loading calculation; where in the parameter P_m is 16.64 MPa, θ is 1.05×10^{-3}sec and the explosive loading time process is as shown in Figure 8.

The full model of the ideal and imperfect stiffened cylindrical shell is adopted for the analysis. Therefore, at the geometrical centre of the finite element model, the Inertia Relief command of ABAQUS uses three shift components u_x, u_y, u_z and three rotational components ϕ_x, ϕ_y, ϕ_z to perform inertial release of pressure loading. The boundary at the peripheral of the fluid will make the shock impact wave to generate refraction or reflection, which will in turn lead to the overlapping or cancelling effect of it with the incident wave in the analysis field. To avoid such phenomenon, during the analysis, the fluid element boundary at the peripheral of the flow field will be set up to be a Non-reflective Boundary, that is, when pressure reaches this boundary, it will all flow out and there will be no reflection. For the intimate contact surface between stiffened cylindrical shell and the fluid, Fluid-Structure Interaction (FSI) condition and ABAQUS Tie commands are used to set the fluid surface and structural surface of this intimate contact surface, to be free of rotational degree of freedom.

4. RESULTS AND DISCUSSION

In this paper, von-Mises stress is used as the shell strength failure judgment reference when a shell takes static water pressure and explosion loading. In the followings, the analysis results will be described at water depths of 50m for

ideal and imperfect stiffened cylindrical shells in terms of standoff point acceleration time history, displacement time history, von Mises stress time history, displacement distribution time history and von Mises stress distribution time history.

4.1 The acceleration time history of Standoff point

In Figure 9 the time history of acceleration change of standoff point under the effect of shock wave at water depth of 50m for ideal and imperfect stiffened cylindrical shell is shown. It can be seen from Figure 9 the maximum acceleration for the ideal and imperfect stiffened cylindrical shell at water depths of 50m all occur at 1.0002s after the start of the explosion. The maximum acceleration of the ideal model is 46,004.2 m/sec^2 and the imperfect model is 60,267.9 m/sec^2. It can be seen that the out-of-round ratio is increased by 2%, but the maximum acceleration of standoff point of the stiffened cylindrical shell increases by about 31%.

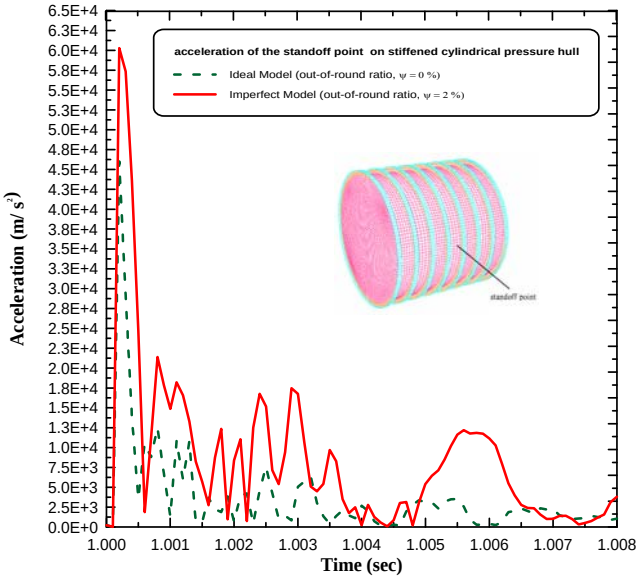

Figure 9. Time history of the acceleration change of the standoff point for ideal and imperfect stiffened cylindrical shell

4.2 Displacement time history of the standoff point

Figure 10 shows the time history diagram of displacement change at the standoff point under the effect of shock wave for ideal and imperfect stiffened cylindrical shell at depths of 50m. It can be seen from Figure 10, the displacement of the standoff point forms a peak shape. The maximum value of the displacement for the ideal model occurs at 1.0032s after the start of the explosion and the imperfect model occurs at 1.0026s. The occurred time of the maximum displacement of the standoff point for the imperfect model is earlier than the ideal model. The maximum displacement of standoff point of the ideal model is 10.4075 mm and the imperfect model is 21.4186 mm. It can be seen that the out-of-round ratio is increased by 2%, the maximum displacement of the standoff point of stiffened cylindrical shell increases by about 105.80%.

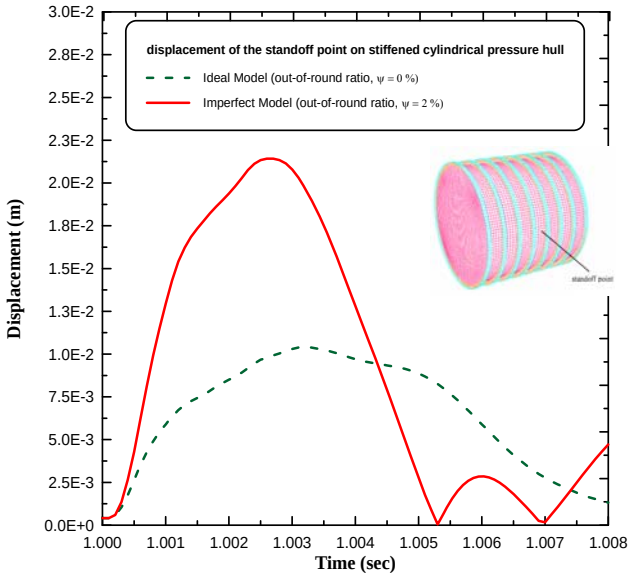

Figure 10. Time history if the displacement change at the standoff point for ideal and imperfect stiffened cylindrical shell

4.3 The von Mises stress time history at the standoff point

The von Mises stress of the standoff point for ideal and imperfect model can be divided into two parts: outer surface stress and inner surface stress. The outer surface is the intimate contact surface between the structure and the fluid and the results are described respectively as in the following:

(1) Time history of the outer surface stress

Figure 11 is the time history diagram of von Mises stress change for the upper surface of standoff point for an ideal and imperfect stiffened cylindrical shell under the action of shock wave at water depths of 50m respectively. It can be seen from Figure 11 that on the outer surface, there

are three peak zones for von Mises stress, which are located respectively at explosive time history of about 1.0007-1.0015s, 1.0025-1.0035s and 1.0055-1.0065s. At the same time, it can be seen that in all the range, due to different out-of-round ratio, the von Mises stress reflected by the shell structure has an obvious difference, that is, the larger the out-of-round ratio, the higher the reflected von Mises stress during the shock wave action period. At water depth of 50m, the maximum von Mises stress of the standoff point for ideal model occurs at 1.0032s with a value of 317.716 Mpa and for the imperfect model occurs at 1.0011s with a value of 641.871 Mpa. It can be seen that the out-of-round ratio is increased by 2%, but the von Mises at the outer surface of the standoff point of the stiffened cylindrical shell increases by about 102.02%.

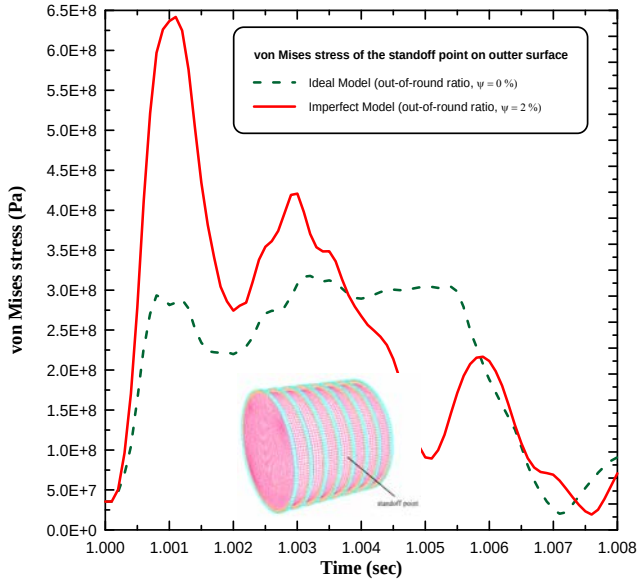

Figure 11. Time history of upper surface von Mises stress change of the standoff point for ideal and imperfect stiffened cylindrical shell

(2) Time history of inner surface stress

Figure 12 is the time history diagram of von Mises stress change for the inner surface of standoff point for an ideal and imperfect stiffened cylindrical shell under the action of shock wave at water depths of 50m respectively.

It can be seen from Figure 12 that there are several peak zones in the inner surface von Mises stress region. The obvious peak zones are located at explosion time history of respectively 1.0007-1.0015s, 1.0045-1.0055s and 1.0075-1.008s. The maximum value of the inner surface von Mises stress of the standoff point for ideal model occurs at 1.0054s with a value of 335.514 Mpa and the imperfect model occurs at 1.0011s with a value of 597.731Mpa. It can be seen that the out-of-round ratio is increased by 2%, but the von Mises at the inner surface of the standoff point of the stiffened cylindrical shell increases by about 78.15%.

It can be seen from the time history of the maximum von Mises stress of the standoff point for the ideal model that the stress level of the inner surface is higher than the stress level of the outer surface. But for the imperfect model that the maximum von Mises stress of the standoff point of the inner surface is lower than the stress level of the outer surface. It can be seen that the external surface (outer surface) stress and non-destructive test of the imperfect cylindrical shell should be performed in a more strict way.

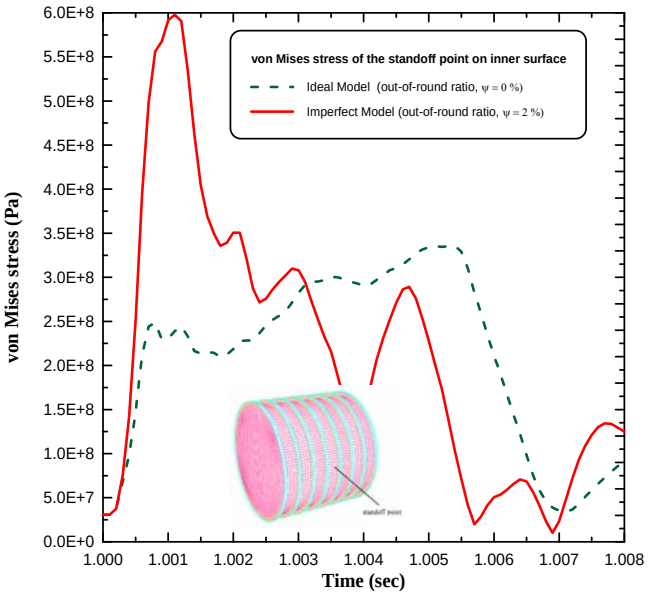

Figure 12. Time history of inner surface von Mises stress change of the standoff point for ideal and imperfect stiffened cylindrical shell

4.4 The time history of maximum von Mises stress change for ideal and imperfect stiffened cylindrical shell

Figure 13 is the time history diagram of maximum von Mises stress change for ideal and imperfect stiffened cylindrical shell under the action of shock wave at water depths of 50m respectively. Figure 14 is the time history

diagram of von Mises stress change for ideal and imperfect stiffened cylindrical shell under the action of shock wave at water depths of respectively.

In the entire explosion reaction history, the HY100 steel material characteristics the yield strength σ_y is 690MPa, ultimate tensile strength is σ_u=793.5 Mpa, we take this as the judgment reference. It can be seen from Figure 13 and Figure 14 that in the initial stage of shock wave action, no matter what the out-of-round ratio is, the maximum von Mise stresses of the cylindrical shell should all exceed the material yield stress but the ultimate stress is not reached. At the same time, the higher the out-of-round ratio, the higher is the maximum von Mises stress.

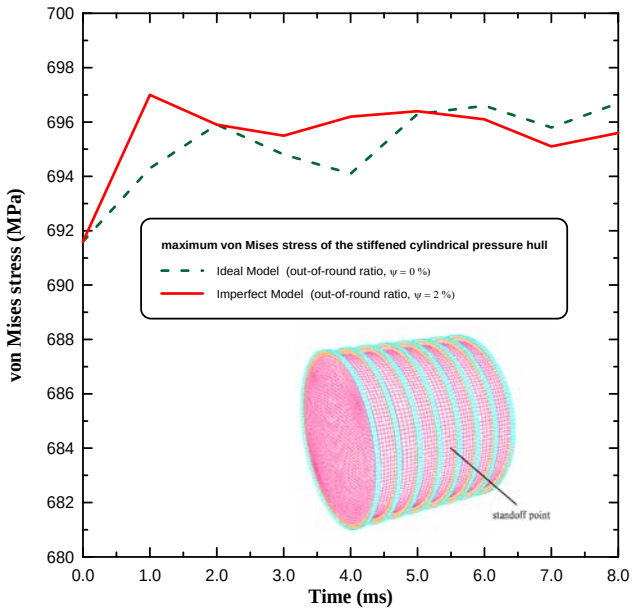

Figure 13. Time history of maximum von Mises stress change of stiffened cylindrical shell for ideal and imperfect stiffened cylindrical shell

4.5 The displacement history for ideal and imperfect stiffened cylindrical shell

Figure 15 is the time history diagram of displacement for ideal and imperfect stiffened cylindrical shell under the action of shock wave at water depths of 50m respectively. It can be seen from Figure 15 that: In the entire explosion reaction history, ideal and imperfect stiffened cylindrical shell with water depth of 50m, the maximum displacement in the shock wave moving direction (x direction) all occur at 5ms-6ms, wherein the maximum displacement of the ideal and imperfect model at water depth of 50m is 19.49mm and 22.16mm. It can be seen that the out-of-round ratio is increased by 2%, but the maximum displacement at x direction of the stiffened cylindrical shell increases by about 13.70%. Therefore, we can understand that the maximum displacement is highly affected by out-of-round ratio of the cylindrical shell.

5. CONCLUSIONS

In this paper, ideal and imperfect stiffened cylindrical shells containing external ribs are used as the target and ABAQUS is used as a tool to study the response of these cylindrical shells at different out-of-round ratios by taking underwater explosion loading with the structure-fluid coupling effect taken into account. The results are summarized in the following:

(1) During the action period of the explosion wave, the maximum acceleration for the ideal and imperfect stiffened cylindrical shell at water depths of 50m all occur at 1.0002s after the start of the explosion. The maximum acceleration of the ideal model is 46,004.2 m/sec^2 and the imperfect model is 60,267.9 m/sec^2. It can be seen that the out-of-round ratio is increased by 2%, but the maximum acceleration of standoff point of the stiffened cylindrical shell increases by about 31%.

(2) During the action period of the explosion wave, the displacement of the standoff point forms a peak shape. The maximum value of the displacement for the ideal model occurs at 1.0032s after the start of the explosion and for the imperfect model occurs at 1.0026s. The occurred time of the maximum displacement of the standoff point for the imperfect model is lesser than the ideal model. The maximum displacement of standoff point of the ideal model is 10.4075 mm and the imperfect model is 21.4186 mm. It can be seen that the out-of-round ratio is increased 2%, the maximum displacement of the standoff point of stiffened cylindrical shell increases by about 105.80%.

(3) On the outer surface, the larger the out-of-round ratio, the higher the reflected von Mises stress, during the shock wave action period. At water depth of 50m, the maximum von Mises stress of the standoff point for ideal model occurs at 1.0032s with a value of 317.716 Mpa and for the imperfect model occurs at 1.0011s with a value of 641.871 Mpa. It can also be seen that the out-of-round ratio is increased by 2%, but the von Mises at the outer surface of the standoff point of the stiffened cylindrical shell increases by about 102.02%.

(4) The maximum value of the inner surface von Mises stress of the standoff point for ideal model occurs at 1.0054s with a value of 335.514 Mpa and the imperfect model occurs at 1.0011s with a value of 597.731Mpa. It can be seen that the out-of-round ratio

is increased by 2%, but the von Mises at the inner surface of the standoff point of the stiffened cylindrical shell increases by about 78.15%.

(5) It can be seen from the time history of the maximum von Mises stress of the standoff point for the ideal model that the stress level of the inner surface is higher than the stress level of the outer surface. But for the imperfect model that the maximum von Mises stress of the standoff point of the inner surface is lower than the stress level of the outer surface. It can be seen that the external surface (outer surface) stress and non-destructive test of the imperfect cylindrical shell should be performed in a stricter way.

(6) In the initial stage of the shock wave action, no matter what the out-of-round ratio is, the maximum von Mise stresses of the cylindrical shell all exceed the material yield stress but the ultimate stress is not reached. At the same time, the higher the out-of-round ratio, the higher is the maximum von Mises stress.

(7) The out-of-round ratio is increased by 2%, but the maximum displacement at x direction of the stiffened cylindrical shell increases by about 13.70%. Therefore, we can understand that the maximum displacement is highly affected by out-of-round ratio of the cylindrical shell.

ACKNOWLEDGEMENT

The authors would like to acknowledge the National Science Council of Republic of China for financially supporting this work under contract NSC 95-2221-E-012-006.

REFERENCES

[1] O. C. Zienkiewicz, R. E. Newton, *Coupled vibrations of a structure submerged in a compressible fluid*. Proc. Int. Symp. Finite Element Techniques, Stuttgart: 359-379, 1969.

[2] M. S. Marcus, *A finite-element method applied to the vibration of submerged plates.* J. Ship Res., 22(2): 94-99, 1978.

[3] H. Huang, K. C. Kiddy, *Transient interaction of a spherical shell with an underwater explosion shock wave and subsequent pulsating bubble*. Shock and Vibration, 2(6): 451-460, 1995.

[4] K. J. Bathe, H. Zhang, M. H. Wang, *Finite element analysis of incompressible and compressible fluid flows with free surfaces and structural interactions.* Comput. Struct., 56(2/3):193-213, 1995.

[5] R. H. Cole, *Underwater Explosive.* Princeton University Press, New York, 1948.

[6] *ABAQUS Theory Manual*, Version 6.7.1, Hibbit, Karlsson, and Sorensen, Inc., Pawtucket, RI, 2007.

[7] R. Kalavalapally, R. Penmetsa, R. Grandhi, *Multidisciplinary optimization of a lightweight torpedo structure subjected to an underwater explosion*, FINITE ELEMENTS IN ANALYSIS AND DESIGN, 43: 103-111, 2006.

[8] *ABAQUS Example Problems Manual*, Version 6.4.1, chap.8.1.4, *Response of a submerged cylinder to an underwater explosion shock wave*. Hibbit, Karlsson, and Sorensen, Inc., Pawtucket, RI, 2003.

[9] Y. S. Tai, S. W. Mao, C.Y. Hsu, *The dynamic response analysis stiffened plates to underwater explosion.* Journal of Taiwan Society of Naval Architects and Marine Engineers, 25(1): 35-46, 2006.

[10] J. F. Zarzour, P. J. Konkol, H. Dong, *Stress-strain characteristics of the heat-affected zone in an hy-100 weldment as determined by microindentation testing.* Materials Characterization, 37: 195-205, 1996.

Time	Ideal Model (ψ=0%)	Imperfect Model (ψ=2%)
1ms	Maximum von Mises stress=694.3MPa 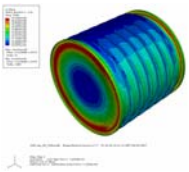	Maximum von Mises stress=697.0MPa 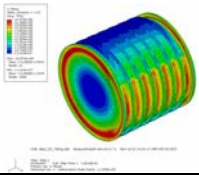
2ms	Maximum von Mises stress=695.9MPa 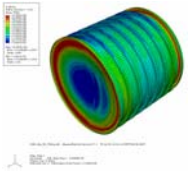	Maximum von Mises stress=696.0MPa 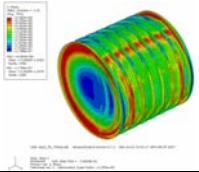
3ms	Maximum von Mises stress=694.8MPa 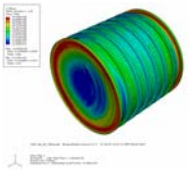	Maximum von Mises stress=695.5MPa 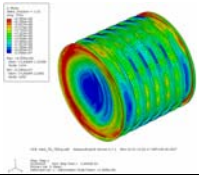
4ms	Maximum von Mises stress=694.1MPa 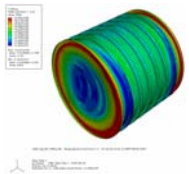	Maximum von Mises stress=696.2MPa 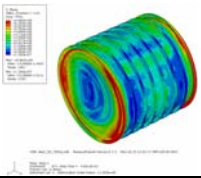
5ms	Maximum von Mises stress=696.3MPa 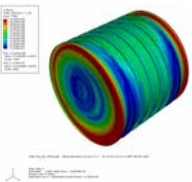	Maximum von Mises stress=696.4MPa 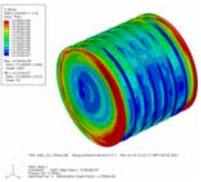
6ms	Maximum von Mises stress=696.6MPa 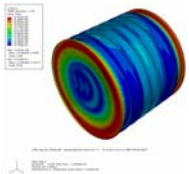	Maximum von Mises stress=696.1MPa 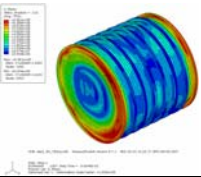
7ms	Maximum von Mises stress=695.8MPa 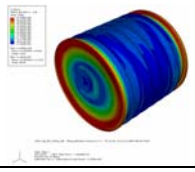	Maximum von Mises stress=695.1MPa 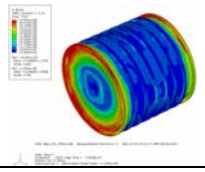
8ms	Maximum von Mises stress=696.7MPa 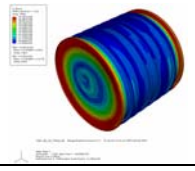	Maximum von Mises stress=695.6MPa 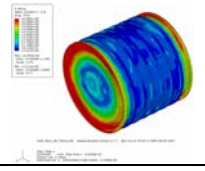

Figure 14. Time history of von Mises stress change for ideal and imperfect stiffened cylindrical shell at water depths of 50m exposed to side-on underwater explosion (TNT = 785Kg)

Time	Ideal Model (ψ=0%)	Imperfect Model (ψ=2%)
1ms	The maximum displacement at x direction =-7.97mm 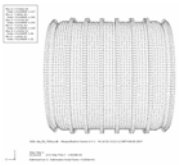	The maximum displacement at x direction =-12.97mm 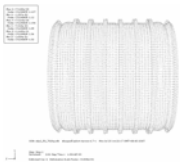
2ms	The maximum displacement at x direction =-9.72mm 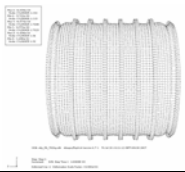	The maximum displacement at x direction =-20.49mm 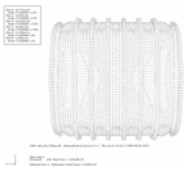
3ms	The maximum displacement at x direction =-11.95mm 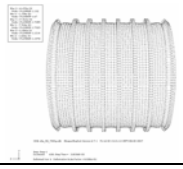	The maximum displacement at x direction =-20.88mm 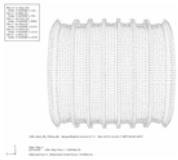
4ms	The maximum displacement at x direction =-16.12mm 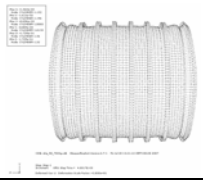	The maximum displacement at x direction =-19.26mm 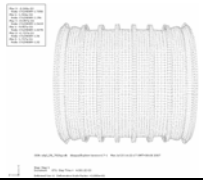
5ms	The maximum displacement at x direction =-18.98mm 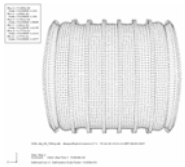	The maximum displacement at x direction =-22.16mm 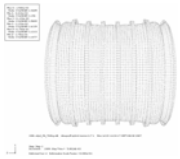
6ms	The maximum displacement at x direction =-19.49mm 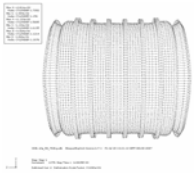	The maximum displacement at x direction =-21.70mm 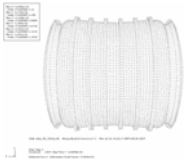
7ms	The maximum displacement at x direction =-18.45mm 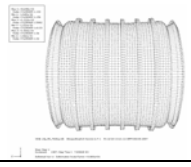	The maximum displacement at x direction =-19.70mm 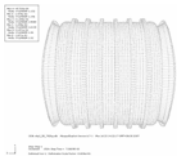
8ms	The maximum displacement at x direction =-17.91mm 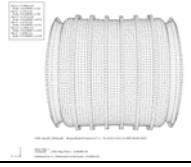	The maximum displacement at x direction =-18.52mm 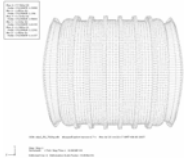

Figure 15. Displacement time history for ideal and imperfect stiffened cylindrical shell at water depths of 50m exposed to side-on underwater explosion (TNT = 785Kg); Note: Deformation scale factor = 30